Title:
Transfinite Surfaces with Optimized Ribbon Cross-Derivatives and Surfaces over Concave Domains

Authors:
Erkan Gunpinar, gunpinar@itu.edu.tr, Istanbul Technical University
A. Alper Tasmektepligil, aalper@yildiz.edu.tr, Yildiz Technical University & Istanbul Technical University
Márton Vaitkus, vaitkus@iit.bme.hu, Budapest University of Technology and Economics
Péter Salvi, salvi@iit.bme.hu, Budapest University of Technology and Economics

Keywords:
Curves and surfaces, Computer-aided design, Transfinite surface interpolation

DOI: 10.14733/cadconfP.2024.205-209

Introduction:

Four-sided tensor-product surfaces are popular in computer-aided geometric design (CAGD) to represent complex free-form objects. Given a curve network representing the feature curves of an object or surrounding smoothly connected surfaces, one of the major challenge in CAGD is to fill a hollow region using a multi-sided surface. Various approaches have been developed to resolve this problem, and each of them comes with its own set of strengths and weaknesses. While trimming is a popular technique to fill the region, feature curves and their associated cross-derivatives cannot be directly manipulated [1]. In contrast to the trimming approaches, feature curves can be directly edited in ribbon-based, multi-sided transfinite surfaces [2, 3, 4] while assuring positional/cross-derivative constraints.

Quality of transfinite surfaces depend not only on the selected interpolation methods but also the user-defined constraints. It has been already demonstrated that automatic setting of cross-derivatives for ribbon-based patches improved the surface quality [5]. -Depending of the magnitudes of the cross-derivatives, the surface obtained goes up or down, and thereby affecting its quality. In this work, we first investigate surface quality (based on Zebra stripes - also known as reflection lines - computed using Rhinoceros 3D[1]) by modifying magnitudes of ribbon cross-derivatives. Ribbon-based transfinite surfaces over concave domains will then be tested.

Transfinite surface optimization:

Given a set of boundary curves with cross-derivatives, a transfinite surface can be interpolated between these curves. In this work, a sphere model is utilized as its geometric properties are already known. Choosing such known example as a test case is advantageous to investigate the interpolated surface quality. Let there be a hexagonal hole on a sphere as shown in Figure 1a, the objective is to fill the hole with a transfinite surface. Ribbon cross-derivatives can be computed using sphere normals and curve tangents (Figure 1b), which are obtained by taking cross product between these two vectors at any curve point.

[1] https://www.rhino3d.com

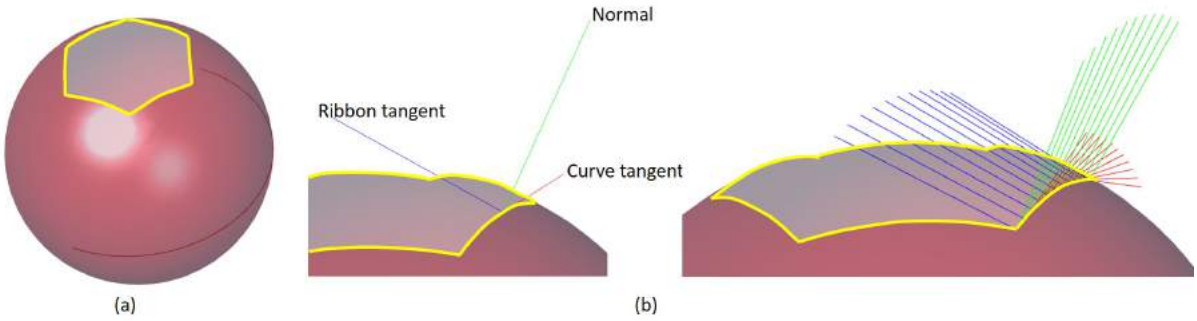

Fig. 1: Given a hexagonal hole on a sphere (a), ribbon cross-derivatives are computed using normal vectors on the sphere and curve tangent vectors.

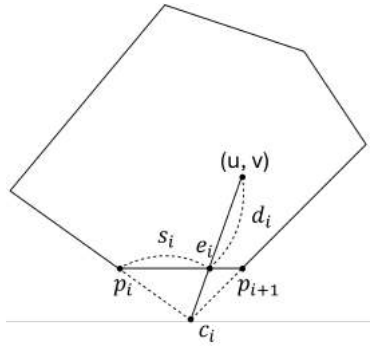

Fig. 2: Computation of radial distance function parameters, (s_i, d_i).

In this work, we use ribbon-based transfinite surfaces, where ribbons, $\{R_i\}$, are bi-parametric surfaces defined in local coordinates (s_i, d_i) by positions, $\{P_i(s_i)\}$, and cross-derivatives, $\{T_i(s_i)\}$, as follows:

$$R_i(s_i, r_i) = P_i(s_i) + d_i T_i(s_i) \tag{2.1}$$

Radial distance function is utilized to compute (s_i, d_i) given (u, v) coordinates (Equation 2.2). The point, e_i, is set by computing the intersection of the domain curve and the line defined by (u, v) and c_i (See Figure 2). Here, c_i denotes the point of intersection when extending the adjacent domain curves.

$$d_i = |(u, v) - e_i| \quad \textit{and} \quad s_i = |e_i - p_i|. \tag{2.2}$$

A special side blending function [7] is utilized to set weights of the ribbons as formulated in Equation 2.3, where $D^n_{i_1,\ldots,i_n} = \prod^n_{i \neq i_1,\ldots,i_n} d_i^2$.

$$\mu_i(d_1, \cdots, d_n) = \frac{D^n_i}{\sum^n_{j=1} D^n_j} \tag{2.3}$$

The blending function is singular at the corner points. Thus, singularity vanishes when two adjacent blending functions are added at the corners (See Equation 2.4).

$$\lim_{\substack{d_{i-1} \to 0 \\ d_i \to 0}} \mu_{i-1}(d_1, d_2, \cdots, d_n) + \mu_i(d_1, d_2, \cdots, d_n) = 1 \tag{2.4}$$

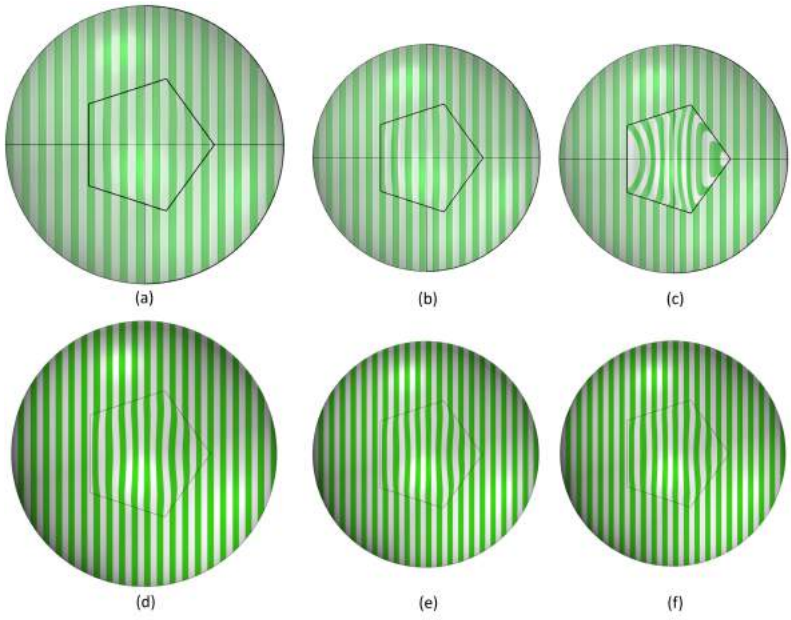

Fig. 3: Zebra stripes of Kato's transfinite surfaces (a-c) and midpoint patches (d-f) with different magnitudes of ribbon cross-derivatives.

Transfinite surface can formally be defined using Equation 2.5.

$$S(u,v) = \sum_{i=1}^{n} R_i(s_i, d_i)\mu(d_1, \cdots, d_n) \tag{2.5}$$

A transfinite surface proposed by Kato [2] is controlled/modified by (1) defining internal constraints (interior control) such as auxiliary vertices and curves [1] and (2) adjusting cross-derivatives [5].

Let $|T_i|$ be the magnitudes of the ribbon cross-derivatives, T_i. We simply adjust magnitudes, $|T_i|$ without changing their directions. Note that cross-derivatives along a ribbon is multiplied by the same multiplier/value.

The quality of the obtained transfinite surfaces are investigated via Zebra stripes. Let $\mathcal{T} = (|T_1|, \ldots,)$ denotes a set of magnitudes for ribbon cross-derivatives. When using Kato's patch to fill a pentagonal hole (on a spherical surface) with $\mathcal{T} = (0.48, 0.55, 0.55, 0.44, 0.58)$, the Zebra stripes were similar to those of a spherical surfaces (i.e., straight from the top view) as shown in Figure 3a. While they were slightly bent when $\mathcal{T} = (0.5, 0.5, 0.5, 0.5, 0.5)$ (Figure 3b). When increasing all magnitudes to 0.75, they were warped more as seen in Figure 3c. Midpoint patch [8] was also utilized[2], where the midpoint was placed at the top of the sphere. Ribbon multipliers controlling the strength of the ribbons were 1.3, 1.4 and 1.5, respectively, for (d), (e) and (f).

The Zebra stripes are shown in Figure 3d, which were bent as well.

Kato and the midpoint patches were further generated for the multi-sided surfaces with different number of sides. Fig. 4 (a) and (c) depict the Zebra stripes when 7 and 10-sided surfaces, where $\mathcal{T} = (0.6137, 0.1934, 0.4527, 0.2277, 0.6085, 0.91, 0.9766)$ and
$\mathcal{T} = (0.6211, 0.5104, 0.3808, 0.9487, 0.3943, 0.6247, 0.5842, 0.8749, 0.4357, 0.5725)$, resp. As the number of

[2] https://github.com/salvipeter/midpoint

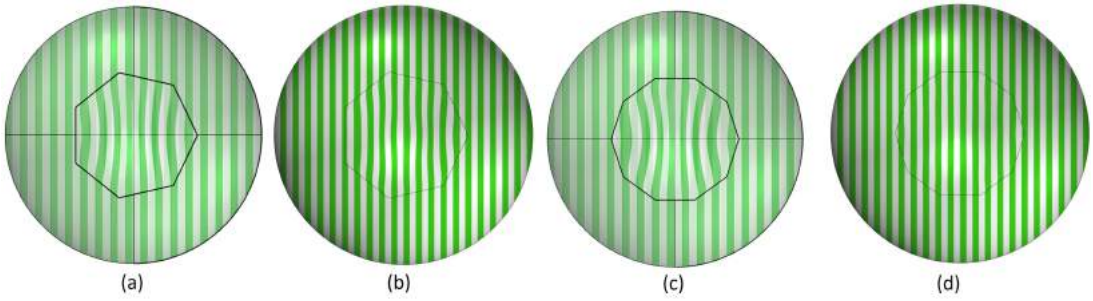

Fig. 4: Zebra stripes for Kato (a, c) and the midpoint (b, d) patches for 7 and 10-sided patches.

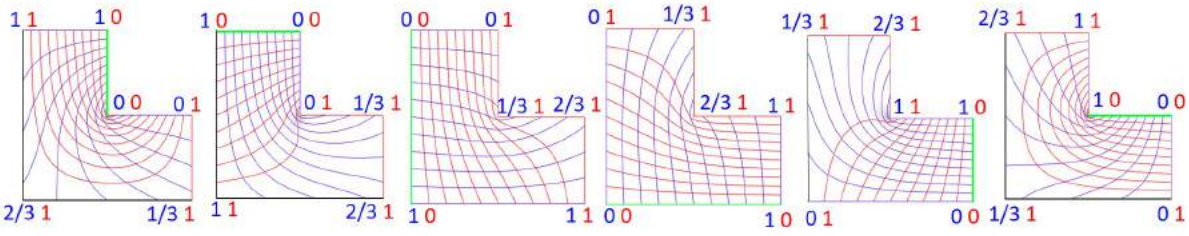

Fig. 5: s and d-curves (blue and red curves) in the domain polygon with s and d values at the corners

.

sides increase, the surface quality deteriorates. Note that the results shown in this work were obtained after randomly generating hundreds of solutions and selecting the one visually having better Zebra stripes. In our experiments, straight Zebra stripes (from the top view) were better as a sphere was utilized as a test case. Fig. 4 (b) and (d) depict the Zebra stripes for midpoint patches with 2.1 and 2.8 of the strength of the ribbons, respectively for (b) and (d). Better surface qualities were obtained for the midpoint patches compared to those of Kato.

Concave domains:

We further investigated the use of Kato's patch [2] over concave domains. Similar to the convex case above, an L shape (Figure 6a) was projected onto a sphere, and ribbon cross-derivatives were then calculated using sphere normals and curve tangents. Domain polygon was obtained by simply projecting the feature curves (red curves in Figure 6a) onto a plane. (s_i, d_i) parameters can then not be computed using radial distance functions as (preceding and subsequent) domain curves adjacent to a domain curve are parallel. Therefore, harmonic functions, constrained minimizers of the Dirichlet energy [9], were utilized to compute (s_i, d_i). Fig. 5 shows s (in blue) and d-curves (in red) for each domain curve (highlighted in green). The values on the corners represent the constraints before computing s and d-values all over the domain. Fig. 6 depict the resulting surface (a) (when $\mathcal{T} = (0.8, 0.8, 0.8, 0.8, 0.8, 0.8)$) and Zebra stripes for this surface (b), which were not that smooth as in the convex case.

Erkan Gunpinar, https://orcid.org/0000-0002-0266-5546
A. Alper Tasmektepligil, https://orcid.org/0000-0001-7429-7247
Marton Vaitkus, https://orcid.org/0000-0003-2064-763X
Peter Salvi, https://orcid.org/0000-0003-2456-2051

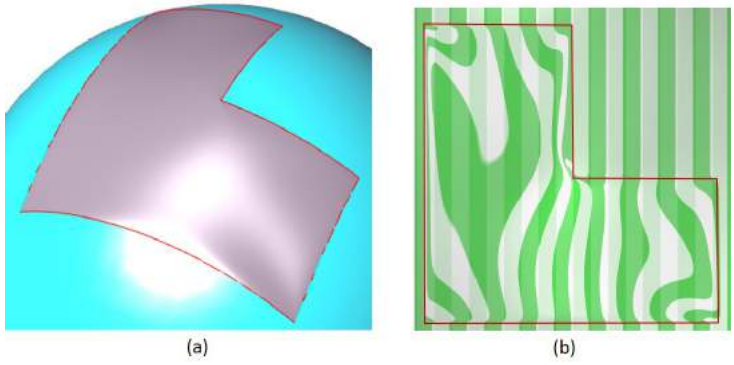

Fig. 6: Transfinite surface obtained (a) and corresponding Zebra stripes (b).

Acknowledgement:
This research was supported by Scientific Research Center of Istanbul Technical University (Project code: 45427).

References:

[1] Varady, T.; Salvi, P.; Rockwood, A.: Transfinite surface interpolation with interior control, Graphical Models, 74(6), 2012, 311-320. https://doi.org/10.1016/j.gmod.2012.03.003

[2] Kato, K.: Generation of N-sided surface patches with holes, Computer-Aided Design, 23(10), 1991, 676-683. https://doi.org/10.1016/0010-4485(91)90020-W

[3] Salvi, P.; Varady, T.; Rockwood, A.: Ribbon-based transfinite surfaces, Computer Aided Geometric Design, 31(9), 2014, 613-630. https://doi.org/10.1016/j.cagd.2014.06.006

[4] Varady, T.; Salvi, P.; Vaitkus, M.: Genuine multi-sided parametric surface patches - A survey, Computer Aided Geometric Design, 110, 2024, 102286. https://doi.org/10.1016/j.cagd.2024.102286

[5] Salvi, P.; Vaitkus, M., Varady, T.: Constrained modeling of multi-sided patches, Computer & Graphics, 114, 2023, 86-95. https://doi.org/10.1016/j.cag.2023.05.020

[6] Farin, G.: Curves and Surfaces for CAGD (Fifth Edition), 16 - Composite Surfaces, The Morgan Kaufmann Series in Computer Graphics, 2002, 285-308. https://doi.org/10.1016/B978-155860737-8/50016-8

[7] Varady, T.; Salvi, P.; Rockwood, A.: Transfinite surface interpolation over irregular n-sided domains, Computer-Aided Design, 43(11), 2011, 1330-1340. https://doi.org/10.1016/j.cad.2011.08.028

[8] Salvi, P.; Kovács, I., Varady, T.:Computationally efficient transfinite patches with fullness control, CoRR, 2020, abs/2002.11212. https://arxiv.org/abs/2002.11212

[9] Vaitkus, M., Varady, T.; Salvi, P.; Sipos, A.: Multi-sided B-spline surfaces over curved, multi-connected domains, Computer Aided Geometric Design, 89, 2021, 102019. https://doi.org/10.1016/j.cagd.2021.102019